2950 Niles Road, St. Joseph, MI 49085-9659, USA
269.429.0300 fax 269.429.3852 hq@asabe.org www.asabe.org

CSBE | SCGAB

An ASABE – CSBE/ASABE Joint Meeting Presentation

Paper Number: 141900251

A Vision Based Sensor for Huanglongbing Disease Detection under a Simulated Field Condition

Alireza Pourreza, PhD Candidate
Agricultural and Biological Engineering, University of Florida, Gainesville, FL 32611, apourreza@ufl.edu

Won Suk Lee, Professor
Agricultural and Biological Engineering, University of Florida, Gainesville, FL 32611, wslee@ufl.edu

Reza Ehsani
Citrus Research and Education Center, University of Florida, Lake Alfred, FL 33850, ehsani@ufl.edu

Written for presentation at the

2014 ASABE and CSBE/SCGAB Annual International Meeting

Sponsored by ASABE

Montreal, Quebec Canada

July 13 – 16, 2014

Abstract. *Florida citrus industry has been suffering from an extremely serious infection, called Huanglongbing (HLB) or citrus greening disease for several years. The disease has been seen in all citrus producing counties in Florida and also some infection has been recently reported in Texas and California. No effective cure has been discovered for this disease yet, still a quick and easy HLB detection method can help citrus growers to remove the infected trees and protect the rest of their groves. Starch accumulation on an infected citrus leaf is one of the HLB symptoms, which create some green islands and yellowish blotch mottles on the leaf. In this study, a new version of a machine vision based sensor was developed which is able to identify the HLB symptomatic leaves under simulated field conditions. The combination of a sensitive monochrome camera and a narrow band polarized illumination system in this sensor could highlight the starch accumulation in HLB infected citrus leaves and differentiate it from yellowish leaves caused by other stresses such as nutrient deficiency. This sensor was examined in both simulated and actual in-field conditions for HLB symptomatic, healthy and nutrient (zinc) deficient leaf samples. Simple statistical histogram features were used for the classification and classification accuracies of over 95% were achieved. Compared to the previous version of our HLB detection system, this approach improved the detection accuracy with a less complicated classification method.*

Keywords. *Citrus Greening, Classification, Disease identification, HLB, Image analysis.*

Introduction

Citrus production plays an important role in Florida's agricultural industry. Over 76,000 people work in the $9 billion citrus industry in Florida. However, this business has always been under the risk of citrus diseases such as citrus canker, citrus greening, and citrus black spot. Huanglongbing (HLB) also called citrus greening is known as the most dangerous citrus disease in the world (Bové, 2006) with no effective cure which was first seen in 2005 in Florida (Halbert, 2005). The statistics showed that the citrus production in Florida significantly decreased after 2005 (Salois et al., 2012) and citrus diseases (including HLB) were the major reason. Although no efficient treatment was reported for this disease, a quick identification and elimination of the affected tree can help to protect the rest of grove from the infection. HLB causes some leaf and fruit symptoms but one of the early symptoms is the appearance of asymmetric yellow shoots on the affected leaf. Etxeberria, Gonzalez, Achor, and Albrigo (2009) showed that the accumulation of starch in an HLB affected leaf which caused the leaf yellowing could be used as an early diagnosis symptom. However, this symptom is comparable to some nutrient deficiencies' symptoms such as zinc deficiency (Gonzalez-Mora, Vallespi, Dima, & Ehsani, 2010) which makes it difficult to be recognized only by a field assessment. Futch, Weingarten, and Irey (2009) showed that the best HLB diagnosis conducted by trained inspectors resulted in an accuracy of 59%.

Sankaran, Maja, Buchanon, and Ehsani (2013) analyzed the visible, near infrared (NIR), and thermal spectral reflectance data to detect the HLB affected citrus trees. They achieved an overall accuracy of 87% using 13 spectral features from the three bands. Aksenov et al. (2014) showed that the volatile organic compounds released from HLB affected trees could be explained using spectrometry methods and be used for diagnosis purpose with the accuracy of ~90%.

Airborne imaging is another vision based diagnosis approach in plant disease identification which was also employed for HLB detection. Li, Lee, Wang, Ehsani, and Yang (2014) introduced an extended spectral angle mapping (ESAM) method for analyzing the airborne hyperspectral images to identify the HLB affected trees. Utilizing this method a classification accuracy of 86% was achieved.

It was shown that the starch accumulation in an HLB affected citrus leaf can be highlighted by narrow-band imaging and a customized use of polarizing filters (Pourreza, Lee, Raveh, Ehsani, & Etxeberria, 2014). The objective of this study aimed to increase the efficiency of the previously introduced approach by developing an improved vision sensor prototype. Enhancing the HLB detection accuracy (especially within the zinc deficient samples), employing a simpler classification algorithm, and adding the capability of on-the-go diagnosis were considered in designing the new prototype.

Materials and Methods

The crystalline structure of starch causes its birefringence characteristic which is the ability of rotating the polarization planar of light in a certain waveband (McMahon, 2004). It was shown that the accumulated starch in HLB affected leaves rotated the planar of polarized light at around 600 nm by 90 degrees (Pourreza, Lee, Raveh, Hong, & Kim, 2013). This feature was used in designing and developing the vision sensor prototype. Figure 1a shows the vision sensor prototype and its components including 10 high power LEDs (LZ4-00A100, 10 W, LED Engin, San Jose, California) at 591 nm powered by 5 LED drivers (RCD-48, 70 W, RECOM, Brooklyn, New York) and a sensitive grayscale camera (DMK 23G445, TheImagingSource, Bremen, Germany).

A total of 60 citrus leaves (20 HLB-negative, 20 HLB-positive, and 20 zinc-deficient) from 'Hamlin' variety were collected in September 2013 from the Citrus Research and Education Center (CREC) grove, University of Florida, Lake Alfred, FL. All samples' HLB statuses were confirmed by a qrt-PCR test which was conducted at the United States Sugar Corporation (USSC), Technical Operations, Southern Gardens (Clewiston, FL).

Sample images were acquired individually (figure 1b) and also in a simulation of in-field condition on an artificial citrus tree. The vision sensor had a customized illumination system and it was designed to acquire images after the sunset for a real in-field experiment. Therefore, for this experiment, the images were acquired in a dark room so that the samples only reflected the polarized light they received from the illumination system of the vision sensor. A fixed distance of 80 cm was used between the sensor and every sample because the reflection of all symptomatic or healthy areas on different type of leaves were within the dynamic range of the camera's sensor with minimum amount of saturated or dark pixels at this distance.

Two basic image descriptors, gray values mean and standard deviation (SD), were extracted from the leaf region in each image and were employed for further analysis.

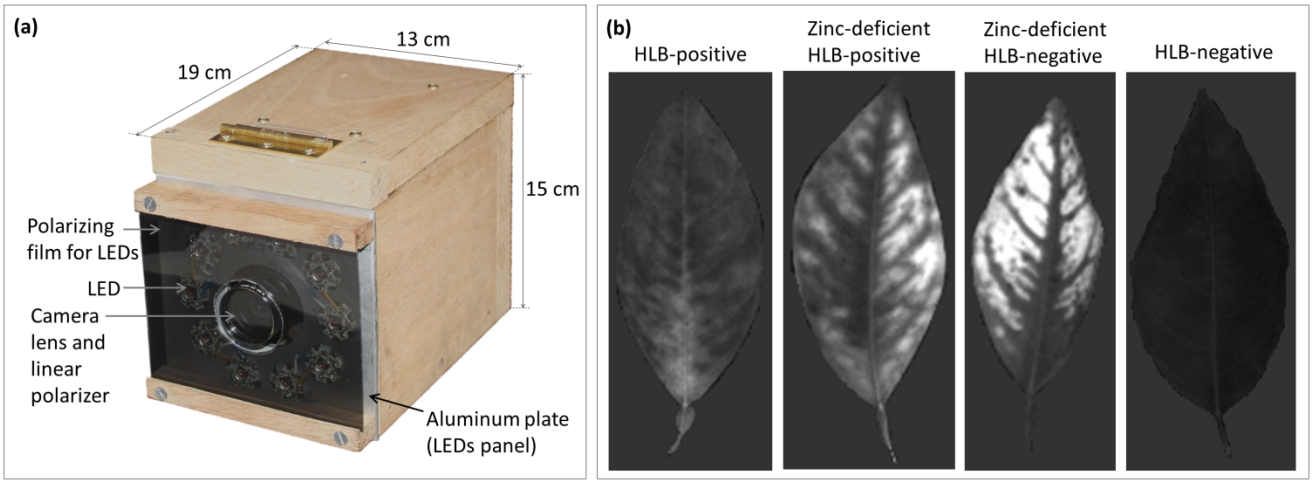

Figure 1. The vision sensor and sample images. (a) The vision sensor prototype including the LEDs, camera, and the polarizing filters as well as the wooden housing and its dimensions. (b) Sample images of citrus leaves in four different classes acquired by the vision sensor.

In order to assess the separability between the four classes, all samples were illustrated in a 2-dimensional scatter plot based on their means (horizontal axis) and SD (vertical axis) features. The optimum threshold between the adjacent pair of classes were obtained by conducting a maximum margin approach (Bishop, 2006). A classification model (figure 2) was designed according to the samples' distribution in the scatter plot in which at each step the input dataset was divided into two sub classes. A support vector machine (SVM) classifier was employed at all classification steps. A K-fold (3-fold) cross validation method was used to confirm that the results were independent to the selection of training and validation data set.

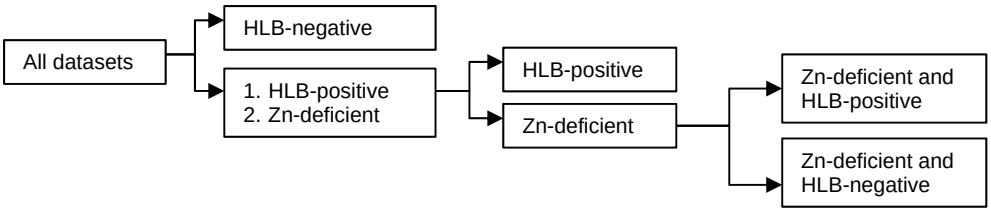

Figure 2. The classification model which was designed based on the scatter plots.

Feature extraction and classification was conducted using MATLAB (version R2011a, MathWorks, Natick, MA) and scatter plots were created in Excel (Microsoft Office, Microsoft, Redmond, Washington).

Results and Discussion

Table 1 includes the gray values means and SDs of HLB-negative, HLB-positive, and zinc-deficient samples. The zinc-deficient class contained two subclasses of 10 HLB-positive and 10 HLB-negative samples. In average, zinc-deficient samples had the greatest means and SDs in both individual leaves and those in an artificial tree datasets, while HLB-negative samples had minimum means and SDs. HLB-negative samples had normal starch content and no zinc deficiency symptoms; therefore, they did not include any high or medium intensity areas. This explains the smaller gray values mean and SDs. HLB-positive samples, on the other hand, had accumulated starch content which caused medium intensity pixel values as well as asymptomatic areas with low intensity. This was the reason for greater means and SDs in HLB-positive class. Zinc-deficient HLB-positive samples contained low intensity (asymptomatic areas), medium intensity (HLB symptomatic areas), and high intensity (zinc deficiency symptomatic areas) pixels which caused the maximum averages of gray values means in both datasets. On the contrary, zinc-deficient HLB-negative samples did not contain any medium intensity (HLB symptomatic areas) pixels; therefore, they had a relatively smaller average mean but a greater average SD because there was a gap in their image histograms between low and high pixel values. Generally, leaves on an artificial tree had smaller gray values and consequently smaller SDs compared to individual leaves. The images of individual leaves were captured at the exact distance of 80 cm, while this distance varied between 79 cm to 82 cm for the leaves on an artificial tree due to the mounting limitation. That was the reason of different feature values for the same samples in two different imaging conditions.

Table 1. The samples features in the both imaging conditions: images of individual leaves, and leaves on the artificial tree.

HLB-negative samples				
ID	μ*		σ**	
	Ind.***	AT****	Ind.	AT
21	38.3	38.1	5.7	8.1
22	28.4	16.8	4.2	3.8
23	49.5	32.0	8.0	4.9
24	26.5	26.1	3.7	5.5
25	20.9	21.5	4.7	4.2
26	26.8	29.2	4.9	4.5
27	28.0	24.1	3.2	3.0
28	26.3	19.4	4.8	3.2
29	23.1	24.6	3.8	4.4
30	23.7	28.2	3.8	5.5
31	35.8	31.1	4.0	4.4
32	34.3	23.9	5.1	3.5
33	30.2	17.5	4.8	2.6
34	29.3	25.9	6.0	4.5
35	33.7	24.9	4.7	3.9
36	26.2	22.7	5.6	3.5
37	31.9	21.9	5.3	4.0
38	36.6	30.8	5.1	4.8
39	41.8	36.7	4.5	6.0
40	34.3	28.6	6.6	4.3
Avg.	31.3	26.2	4.9	4.4

HLB-positive samples				
ID	μ		σ	
	Ind.	AT	Ind.	AT
41	48.5	37.9	14.8	13.6
42	51.5	33.6	14.9	10.0
43	78.7	48.3	38.9	20.5
44	59.7	51.3	18.8	17.1
45	63.8	57.3	26.9	24.6
46	49.3	56.8	13.6	14.2
47	46.2	41.2	12.7	9.7
48	53.4	36.9	13.5	9.6
49	52.2	54.2	23.7	22.8
50	51.8	54.4	15.6	16.0
51	81.2	75.9	23.0	23.6
52	47.8	36.9	21.1	14.4
53	56.1	41.3	18.7	14.1
54	76.0	62.7	17.8	13.9
55	57.5	45.7	11.0	8.2
56	64.1	60.3	17.3	15.0
57	69.0	45.4	15.5	10.2
58	103.5	89.6	39.9	34.4
59	47.8	52.9	12.1	13.4
60	52.9	43.2	18.4	12.0
Avg.	60.6	51.3	19.4	15.9

Zinc-deficient samples				
Zinc-deficient HLB-negative				
ID	μ		σ	
	Ind.	AT	Ind.	AT
1	84.7	55.4	65.8	35.2
3	110.3	79.3	65.7	52.7
4	89.4	114.5	58.6	66.2
5	107.9	104.7	58.6	51.9
7	121.4	112.2	85.4	78.8
10	127.5	122	77.5	71.8
12	119.4	111.1	82.2	71.6
15	98	77.3	55.3	41.1
16	128.6	108.6	69.2	61.4
17	89.3	65.9	63.7	40.3
Avg.	107.65	95.1	68.2	57.1
Zinc-deficient HLB-positive				
2	100.4	71.5	42.6	31.1
6	114.8	119.6	37.1	49.1
8	121	86.9	44.1	38.2
9	213.8	212.9	59	50.3
11	102.9	92	62.4	57.5
13	140.9	93.4	65.7	53.7
14	134.5	111.3	64.3	53.3
18	98.7	85.6	44.5	36.8
19	162.1	159.1	64.5	65.5
20	162.3	149.7	49.7	45.1
Avg.	135.14	118.2	53.39	48.06

* μ : The mean of the gray values
** σ : The SD of the gray values
*** Ind. : Images of individual leaves
**** FA : Images of leaves on an artificial tree

Figure 3 shows the two dimensional scatter plots of samples according to their gray values mean and SDs. The dashed lines in each plot indicate the thresholds between the adjacent pair of classes which were obtained using the maximum margin method. The three thresholds in the individual leaves dataset (figure 3a) separated the four classes with only two mis-clustered samples. The number of mis-clustered samples increased to four for the leaves on an artificial tree dataset. The samples which are specified with a circle were the support vectors defining the possible margins of each class.

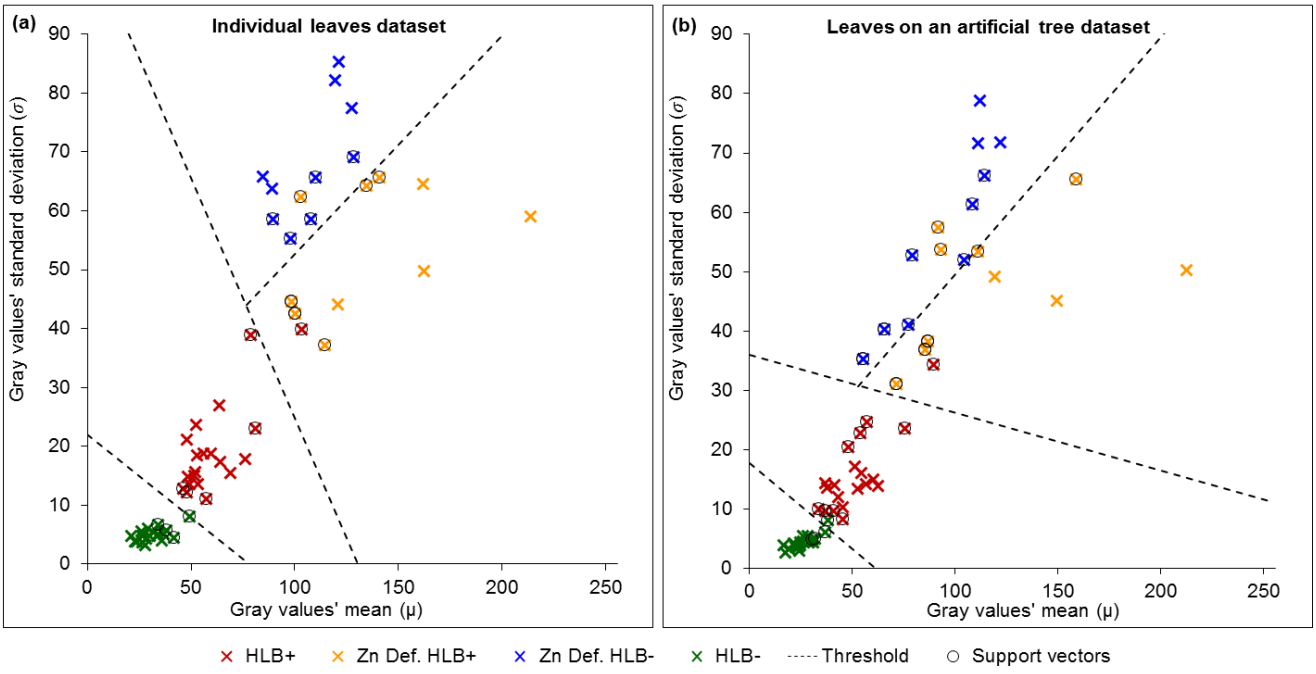

Figure 3. Illustration of samples in a two dimensional scatter plot based on their gray values mean and SD: (a) samples in individual leaves dataset, and (b) samples in leaves on an artificial tree dataset.

Although, it seems a customized threshold drawn by visual observation can perform a better separation in some cases, but using maximum margin method provided a more general separation with less dependency to a specific dataset.

Figure 4 shows the classification and misclassification rates for each class in two datasets. Samples in HLB-negative and zinc-deficient HLB-negative classes were classified with the accuracy of 100% in both datasets. Also over 95% of HLB-positive samples were correctly classified in both datasets. Few HLB-positive samples within the zinc-deficient class were misclassified in zinc-deficient HLB-negative class. Overall accuracies of 97% and 95.5% were achieved using the introduced classification model for individual leaves and leaves on an artificial tree datasets, respectively. Only two simple image descriptors and SVM classifier were employed for identification purpose which resulted in a significantly better accuracies compared to our previous study.

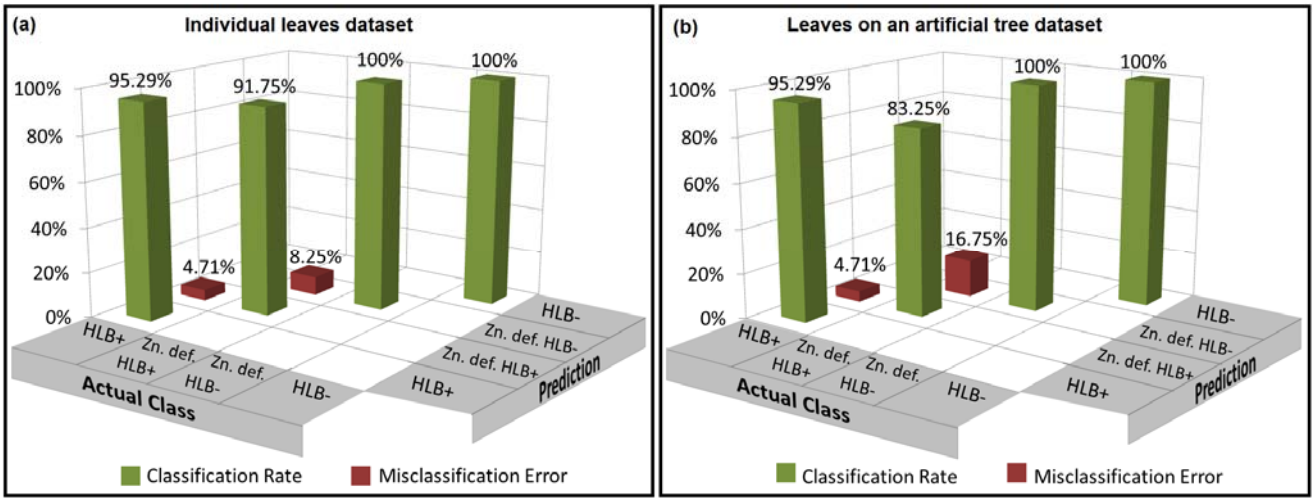

Figure 4. Classification and misclassification rates achieved using the classification model: (a) classification results in individual leaves dataset, and (b) classification results in leaves on an artificial tree dataset.

Conclusion

In this study, an optimized HLB detection approach was introduced and its performance in a simulation of the in-field condition was assessed. The approach had clear advantages compared to other methods. The vision sensor was developed with inexpensive items which makes it an affordable diagnosis solution for every citrus grower. Not only is this sensor able to identify the HLB symptomatic area, but also it is able to differentiate the zinc deficiency from HLB infection. No sample collection and preparation is required for this method and the sensor can be used for an on-the-go diagnosis application. The results of this research showed that the proper use of narrow band illumination and polarizing filters could enhance the accuracy and simplify the identification algorithm.

Acknowledgements

The authors would like to acknowledge the Citrus Research and Development Foundation (CRDF) for financially support this research. We would also like to thank Mr. Michael Irey (United States Sugar Corporation, Clewiston, FL) for his contribution in this study.

References

Aksenov, Alexander A, Pasamontes, Alberto, Peirano, Daniel J, Zhao, Weixiang, Dandekar, Abhaya M, Fiehn, Oliver, Davis, Cristina E. (2014). Detection of Huanglongbing Disease Using Differential Mobility Spectrometry. *Analytical chemistry, 86*(5), 2481-2488.

Bishop, Christopher M. (2006). *Pattern recognition and machine learning* (1st ed.). New York: Springer Science.

Bové, Joseph M. (2006). Huanglongbing: a destructive, newly-emerging, century-old disease of citrus. *Journal of plant pathology, 88*(1), 7-37.

Etxeberria, Ed, Gonzalez, Pedro, Achor, Diann, & Albrigo, Gene. (2009). Anatomical distribution of abnormally high levels of starch in HLB-affected Valencia orange trees. *Physiological and Molecular Plant Pathology,*

74(1), 76-83.

Futch, STEVE, Weingarten, SHAWRON, & Irey, MIKE. (2009). *Determining HLB infection levels using multiple survey methods in Florida citrus.* Paper presented at the Proc. Fla. State Hort. Soc.

Gonzalez-Mora, Jose, Vallespi, Carlos, Dima, Cristian S, & Ehsani, Reza. (2010). HLB detection using hyperspectral radiometry. *10th ICPA Proceedings. Available from:< http://www. andrew. cmu. edu/user/jlibby/robotany/Gonzalez-Mora-2010. pdf*.

Halbert, S.E. (2005). *The discovery of Huanglongbing in Florida.* Paper presented at the 2nd International Citrus Canker and Huanglongbing Research Workshop, Orlando, Florida.

Li, Han, Lee, Won Suk, Wang, Ku, Ehsani, Reza, & Yang, Chenghai. (2014). 'Extended spectral angle mapping (ESAM)'for citrus greening disease detection using airborne hyperspectral imaging. *Precision Agriculture, 15*, 162-183.

McMahon, K.A. . (2004). Practical botany - the Maltese cross. *Tested Studies for Laboratory Teaching, 25*, 352-357.

Pourreza, Alireza, Lee, Won Suk, Raveh, Eran, Ehsani, Reza, & Etxeberria, Edgardo. (2014). Citrus Huanglongbing Disease Detection Using Narrow Band Imaging and Polarized Illumination. *Trans. ASABE 57*(1), 259-272.

Pourreza, Alireza, Lee, Won Suk, Raveh, Eran, Hong, Youngki, & Kim, Hyuck-Joo. (2013). *Identification of citrus greening disease using a visible band image analysis*. Paper presented at the ASABE Annual International Meeting, Kansas City, Missouri. http://elibrary.asabe.org/abstract.asp?adid=43724&t=5

Salois, Matthew J. , Jauregui, Carlos, Ferrell, Lori, Norberg, Robert P., Barnhardt, Valerie, & Griffith, Toni. (2012). *Citrus reference Book*. Gainesville, Florida: Florida Department of Citrus.

Sankaran, Sindhuja, Maja, Joe Mari, Buchanon, Sherrie, & Ehsani, Reza. (2013). Huanglongbing (Citrus Greening) Detection Using Visible, Near Infrared and Thermal Imaging Techniques. *Sensors, 13*(2), 2117-2130.